Fatigue design for timber and wood-based materials

STEP lecture E22
M.P. Ansell
University of Bath

Objectives

The lecture explains the nature of constant amplitude and complex fatigue loads, examines methods for establishing the fatigue characteristics of wood, describes life prediction techniques for the fatigue design of timber and wood-based materials and outlines property changes which occur in fatigue.

Summary

The introduction explains basic fatigue terminology and describes fatigue loading configurations. The lives of wood-based materials subjected to fatigue at constant amplitude are represented by σ-N (stress versus number of cycles to failure) or ε-N (strain versus number of cycles to failure) curves which vary with the R ratio, which is the ratio of the minimum cyclic stress to the maximum cyclic stress. Constant life diagrams may be constructed from such curves and relationships such as the Goodman equation describe the form of the constant life lines. The prediction of fatigue life under complex loading conditions, for example a wind or vehicle load, is achieved by a cycle counting technique which separates the load spectrum into cycles of mean stress and stress amplitude. This information is combined with constant life information and a fatigue life prediction is achieved by performing a simple Miner's Rule summation. The fatigue design approach is being applied routinely in the development of wood composite wind turbine blades. The lecture concludes by describing the microstructural damage caused by fatigue stresses in wood.

Introduction

Wooden structures are frequently subjected to dynamic loads, for example vehicle loads acting on factory floors and bridges and wind loads acting on timber roofs. These fatigue loads often cause sub-critical, microstructural damage which under more extreme conditions may lead to fatigue failure. Fatigue failure of materials occurs following the application of cyclic stress (or strain) with a peak value which is less than the static strength (or strain at failure) of the material. Laboratory fatigue tests which last for less than 10^4 cycles are known as low cycle fatigue tests whereas those which last longer are termed high cycle tests.

The fatigue loading mode, eg. tension, compression, shear, torsion or mixed mode, Figure 1, affects the fatigue life and the failure mechanism. Metal alloys are susceptible to tensile fatigue, especially at welds and notches which results in fatigue crack propagation. Wood is much less sensitive to tensile fatigue for propagation modes across the grain and fatigue damage occurs by microstructural damage events throughout the volume of the wood, unless joints or defects initiate localised damage. Hence it is not appropriate to apply fracture mechanics to fatigue in a tensile crack opening mode across the grain, although the Paris law can be applied to crack opening modes along the grain. The Paris Law is an empirical law which describes the rate of steady state crack propagation in fatigue where,

$$\frac{da}{dN} = C\,\Delta K^{m} \qquad (1)$$

where a is the crack length, N is the number of cycles, C and m are materials constants and ΔK is the critical stress intensity range.

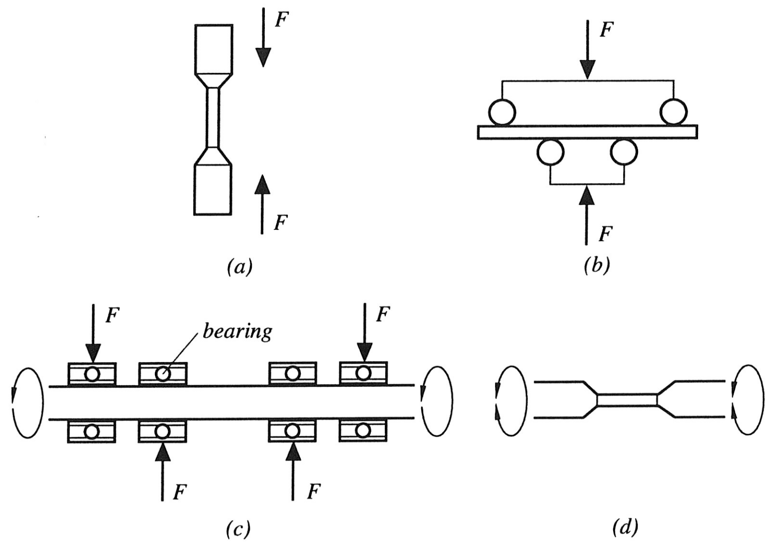

Figure 1 *Fatigue loading configurations. (a) Axial, (b) bending, (c) combined torsional and bending, (d) torsional.*

Fatigue design methods described in this lecture have been applied to solid wood and to unidirectional laminated veneer lumber (LVL) loaded along the grain.

σ-N (S-N) curves and the R ratio

The fatigue life of engineering materials is traditionally represented in the form stress-life (σ-N or S-N) or strain-life (ε-N) curves following Wöhler's (1867) classic work on iron railway axles in the 1850s and 1860s. The stress (stress-controlled test) or strain (strain-controlled test) can refer to the peak value, the amplitude or the range. For the sake of simplicity σ-N tests are referred to from now on. Sinusoidal or sawtooth stresses may be applied to test pieces but it is necessary to identify the loading configuration and whether the load is repeated, reversed or of variable amplitude. The waveform presented in Figure 2 depicts a repeated tensile stress.

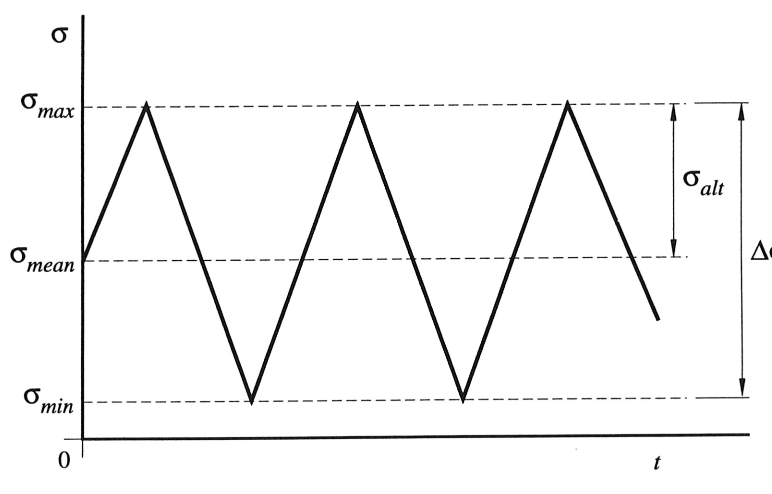

Figure 2 *Sawtooth stress versus time waveform illustrating characteristic stresses.*

The characteristic stresses are defined as follows:

The stress range, $\Delta\sigma = \sigma_{max} \; \sigma_{min} = 2\sigma_{alt}$

The mean stress, $\sigma_{mean} = 0{,}5\ (\sigma_{max} + \sigma_{min})$

The alternating stress, $\sigma_{alt} = 0{,}5\ (\sigma_{max} - \sigma_{min})$

The *R* ratio, $R = \sigma_{min}/\sigma_{max} = (\sigma_{mean} - \sigma_{alt})/(\sigma_{mean} + \sigma_{alt})$.

The *R* ratio is a key to understanding the loading mode in tests involving combinations of tensile and compressive stresses, for example, $R = -1$ represents reversed loading. Figure 3 illustrates some typical *R* ratios where σ_{min} is always taken to be the most negative stress.

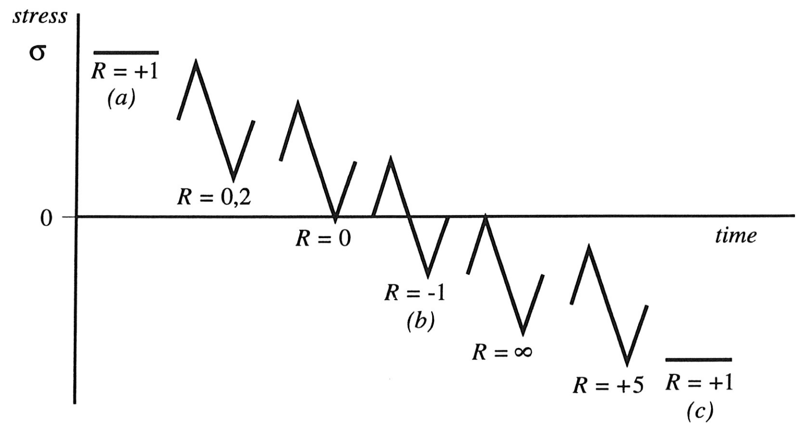

Figure 3 *Single stress cycles depicting typical R ratios. (a) static tension, (b) reversed loading, (c) static compression.*

Other than static tensile and compressive stresses, where *R* is equal to one, the *R* ratio identifies the fatigue loading mode as follows:

$R = 1$ to 0	Tension-tension.
$R = 0$ to -1	Tension-compression.
$R = -1$ to $\pm\infty$	Compression-tension.
$R = \pm\infty$ to -1	Compression-compression.

The reader should ponder carefully the mode transitions at $R = 0$ and $\pm\infty$. At $R = -1$ the loading is reversed and $\sigma_{alt} = \sigma_{max} = -\sigma_{min}$. Wood and wood composites are evaluated at *R* ratios which most usefully simulate loading in the engineered product. In order to fully evaluate wood composites in fatigue they should be tested at several *R* ratios which will result in a set of σ-*N* curves, Figure 4, which are usually plotted in a linear stress versus log cycles form. Similar graphs have been published by Tsai and Ansell (1990) and Bonfield and Ansell (1991) for flexural and axial fatigue, respectively, of wood composites.

The schematic diagram represents regression lines through a scatter of fatigue failure points (not shown) at five *R* ratios and static strength values at one quarter of a cycle (log $N = -0{,}6$). Bearing in mind that stress is the independent variable and that log cycles to failure is the dependent variable, it is important that the regression analysis should be performed on data in log N-σ form. It may then be plotted in the traditional σ-log N format. Figure 4 demonstrates that as the *R* ratio approaches 1 (static stress) the fatigue life increases and that reversed loading results in the shortest fatigue lives. The fatigue life of wood decreases as the moisture content increases (Tsai and Ansell, 1990).

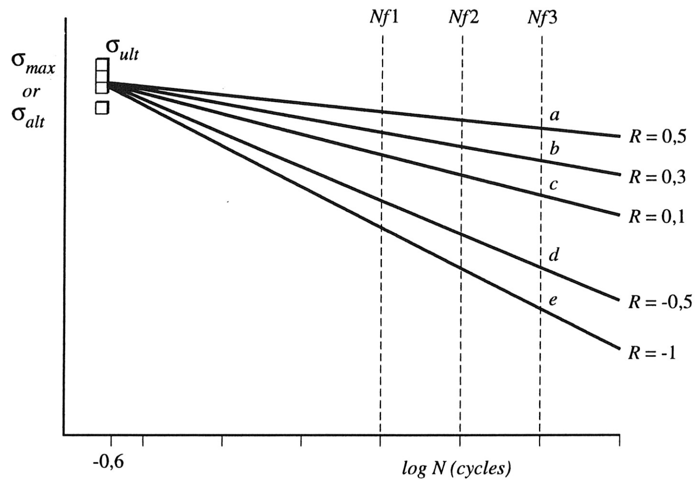

Figure 4 *Set of σ -log N curves for tension-tension (R = 0,1, 0,3 and 0,5) and tension-compression (R = -0,5 and -1) cyclic stress configurations.*

At this point it is worth mentioning the overriding importance of the difference between the mean static tensile strength of wood and the mean static compressive strength. Whilst the static strength in tension is considerably greater than that in compression the slope of the σ-log *N* curves in tension-tension is considerably greater than in compression-compression. In other words wood is remarkably fatigue resistant in compression-compression until σ_{max} approaches the static compressive strength. Once loading becomes mixed mode (R = -1 to ±∞) the tensile component of loading alters the mechanism of fatigue damage accumulation.

Constant life lines

It is useful to be able to predict the fatigue life of wood at any *R* ratio by interpolation from σ-log *N* data at any *R* ratio. This is achieved by plotting constant life or Goodman diagrams, such as Figure 5, using the σ-*N* data from Figure 4. The lines depicted radiating from the origin are lines of constant *R* ratio because the constant ratio $\sigma_{min}/\sigma_{max}$ is equal to the ratio $\sigma_{alt}/\sigma_{mean}$.

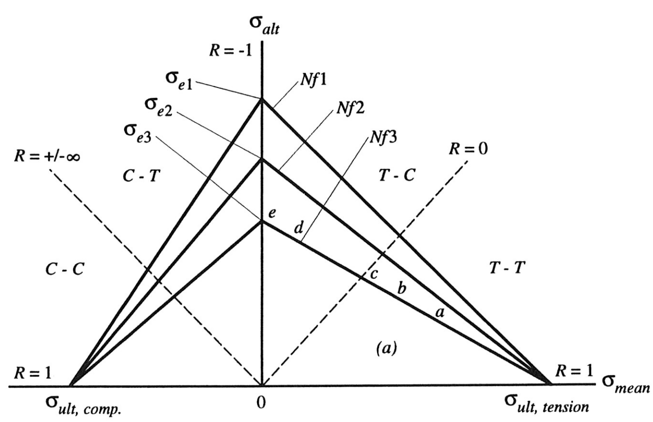

Figure 5 *Set of constant life lines for combinations of alternating and mean stresses resulting in constant lives of Nf1, Nf2 and Nf3 cycles. (a) Safe combination of stresses below constant life line.*

In Figure 4 each vertical line $Nf1$, $Nf2$, $Nf3$, representing chosen constant lives, intersects the σ-N curves for the R ratios 0,5, 0,3, 0,1, -0,5 and -1. The intersection points a, b, c, d, and e for a constant life $Nf3$, for example, can be represented as corresponding points on the constant life diagram, Figure 5, through which the constant life line can be drawn. The values $\sigma e1$, $\sigma e2$ and $\sigma e3$ represent the alternating stress values for which constant lives of $Nf1$, $Nf2$, $Nf3$ are achieved respectively. The area under each constant life line represents combinations of mean and alternating stress which will not result in fatigue failure at cycle totals less than the constant life.

The Goodman equation for the constant life line on the tension side of the constant life diagram is represented as,

$$\sigma_{alt} = \sigma_e \left[1 - \frac{\sigma_{mean}}{\sigma_{ult,\ tension}} \right] \tag{2}$$

for constant life points which fall on a straight line. Other versions of this equation are possible, including the following:

Gerber

$$\sigma_{alt} = \sigma_e \left[1 - \left(\frac{\sigma_{mean}}{\sigma_{ult,\ tension}} \right)^2 \right] \tag{3}$$

Factored Goodman

$$\sigma_{alt} = \frac{\sigma_e}{M} \left[1 - \left(\frac{\sigma_{mean}}{\sigma_{ult,\ tension} / M} \right) \right] \tag{4}$$

The Gerber equation represents a parabolic constant life line with the same limits as the Goodman line. The factored Goodman equation includes a safety factor $M > 1$ which reduces the area under the Goodman line.

Wood species tested to date (Bond et al., 1993) obey Goodman relationships and two equations are required to characterize each side of the constant life diagram, (*C-C/C-T* and *T-C/T-T*). Constant life diagrams for wood are also very similar in form to those for fibre-reinforced plastics (Ansell et al., 1993). It is clear that the constant amplitude fatigue life at any R ratio and peak stress can be interpolated from constant life diagrams of the form depicted in Figure 5. Furthermore it is only necessary to measure the static tensile and compressive strengths and to obtain the σ-N curve at R = -1 to obtain the two Goodman relationships for each side of the constant life diagram, which significantly reduces time spent in fatigue testing.

Complex loads and life prediction

When wood is subjected to fatigue stresses in the field it is often the case that stresses are complex (variable amplitude) rather than constant amplitude. High amplitude cycles will cause the most fatigue damage. Wood is a linear-elastic material up to a proportional limit, illustrated in somewhat exaggerated form in Figure 6, but it is usually strained to levels well below the elastic limit. However it is essential to appreciate that during fatigue wood dissipates progressively more energy through hysteresis (Hacker and Ansell, 1994) as microstructural damage accumulates, following visco-elastic and plastic deformation.

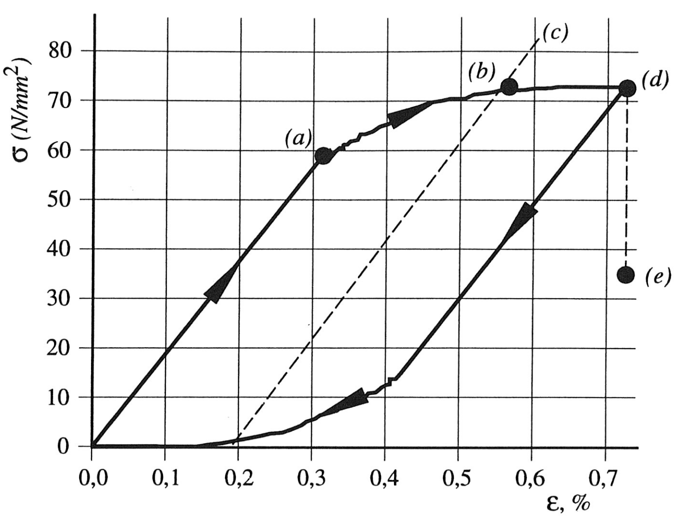

Figure 6 *Stress versus strain hysteresis loop. (a) proportional limit, (b) yield stress, (c) 0,2% offset, (d) tensile strength, (e) design tensile strength.*

In order to predict fatigue life under complex load a simple summation rule such as that due to Palmgren-Miner is used,

$$\sum_{1}^{i} \frac{n_i}{N_i} = 1 \tag{5}$$

where n_i is the number of cycles of stress experienced that result in failure after N_i cycles. The complex spectrum can be split into individual cycles which are sorted into "bins" (data stores), labelled by mean stress (or strain) and range stress (or strain), by the use of a suitable counting technique in order to estimate the proportion of fatigue life used up. Rainflow counting is an appropriate technique for binning cycle counts and this method is illustrated, with reference to hysteresis, in Figure 7. (The term "rainflow" relates to the concept of rain flowing down the series of roofs represented by Figure 7(a) which is used to define loading cycles. This is difficult to visualise and is avoided in this account).

The strain-time (or stress-time) history *ABCDEDFGA* is part of a complex spectrum which corresponds to a stress-strain hysteresis loop containing three sub-loops, two of which are elastic and one of which is elastic-plastic. Loading from *A* to *B* involves elastic and plastic deformation and the unloading from *B* to *C* is elastic. Subsequent loading from *C* to *D* exceeds the strain level experienced at *B* so this stage involves elastic (from *C* to *B*) and plastic (from *B* to *D*) deformation. Unloading from *D* to *E* returns the state of strain elastically to the same strain as at *C* but the stress level has changed due to the plastic deformation experienced. Returning the strain to *D* after a small amount of inelastic relaxation has occurred closes the hysteresis loop *DED*.

Finally the strain returns to *A* via the elastic loop *FGF*. Two open hysteresis loops remain, *ADA* and *DED*, where elastic and plastic deformation occurred, and two closed loops *BCB* and *FGF* where only elastic deformation occurred. These loops are recorded and binned in terms of their mean and range strain or stress. Each loop is related via the constant life diagram to the σ-*N* curve for the associated mean and range stress using appropriate computer software. The accumulated number of cycles for all loops are summed using the Palmgren-Miner rule and the fatigue life can be predicted in terms of the number of passes through the load-time history.

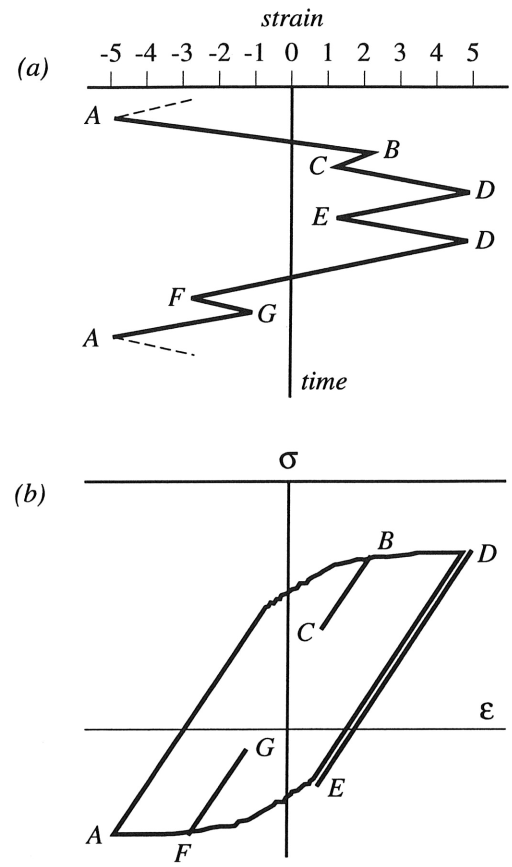

Figure 7 *Diagram demonstrating the Rainflow Counting technique. (a) Complex load-time history, (b) stress-strain hysteresis loop.*

Fatigue evaluation of wood composites for wind turbine blades

Recent fatigue research on wood has been driven by the design of wind turbine blades of up to 45 *m* diameter constructed from LVL, (Ansell et al., 1991). This work has involved the evaluation of several wood species and the performance of joints (Bonfield et al., 1992). The problems associated with using wood composites in offshore wind farm locations has also been addressed (Bond and Ansell, 1993).

Fatigue damage and property changes in wood

Microstructural evidence for fatigue damage in Sitka spruce in four point bending has been observed by Tsai and Ansell (1990). On the compression side of the specimen damage is initiated in the double tracheid wall of the softwood by cell wall buckling, observed by polarised light optical microscopy. As fatigue cycling continues diagonal arrays of buckled zones develop across many adjacent cells until cell buckling occurs and visible compression creases form at the compression surface. The neutral axis of the wood beam moves towards the tensile surface, increasing the load on this face, and the first manifestation of beam failure is jagged tensile fracture. Hacker et al. (1994) have reported on the dynamic mechanical property changes that occur in compression-compression, tension-tension and reversed loading experiments. Changes in the dynamic modulus, hysteresis loop area, underlying creep strain and the fatigue modulus are described.

References

Ansell, M.P., Hancock, M. and Bonfield, P.W. "Wood composites - the optimum fatigue resistant materials for commercial wind turbine blades". In the Proceedings of the International Timber Engineering Conference, London, 4.194-4.202, September 1991.

Ansell, M.P., Bond, I.P. and Bonfield, P.W., "Constant life diagrams for wood composites and polymer matrix composites", Proceedings of the Ninth International Conference on Composite Materials (ICCM-9), Madrid, Spain, ed. Miravete, Antonio, Pub. University of Zaragoza, Woodhead Publishing Ltd., V, 692-699, 1993.

Bond, I.P., Ansell, M.P. and Hacker, C.L., "Fatigue testing of wood composites for aerogenerator rotor blades. Part VIII. Statistical treatment of constant life data for design optimization", Proceedings of the 1993 European Community Wind Energy Conference, Lübeck-Travemünde, Germany, Pub. H.S. Stephens and Associates, 137-140, 1993.

Bond, I.P. and Ansell, M.P., "Effect of the marine environment on the fatigue life of wind turbine materials", Wind Engineering, 17, 2, 100-107, 1993.

Bonfield, P.W. and Ansell, M.P., "The fatigue properties of wood in tension, compression and shear". J. Mat. Sci., 26, 4765-4773, 1991.

Bonfield, P.W., Bond, I.P., Hacker, C.L. and Ansell, M.P., "Fatigue testing of wood composites for aerogenerator rotor blades. Part VII. Alternative wood species and joints", in "Wind Energy Conversion 1992", ed. Clayton, B.R. Pub. Mechanical Engineering Publications Ltd, 243-250, 1992.

Hacker, C.L. and Ansell, M.P. "Stress-strain hysteresis loop capture in the assessment of fatigue damage accumulation in wood composites". To be published in the Proceedings of EWEC '94, the European Wind Energy Association Conference, Thessaloniki, Greece, 1994.

Tsai, K.T. and Ansell, M.P., "The fatigue properties of wood in flexure". J. Mat. Sci., 22, 865-878, 1990.

Wöhler, M., "Wöhler's experiments on the strength of metals", Engineering, Aug. 23, 1867.